has a significant temperature dependence.

Because the nature of tropospheric aerosols varies greatly with time, location, and other atmospheric constituents, characterization is extremely complex. If we take typical data from a polluted atmosphere, such as the Los Angeles basin, we calculate a gas kinetic collision frequency between a molecule and an aerosol particle of ~ 1 sec^{-1} (*5*). These aerosols are known to contain significant concentrations of H_2SO_4. We would therefore predict a heterogeneous loss rate constant of $\sim 10^{-5}$ sec^{-1} for most of the species in the upper half of Table 1 (*6*). Comparison with typical photolysis rate constants (per second) (N_2O_5, 10^{-5}; H_2O_2, 10^{-5}; and HNO_3, 10^{-6}) indicates that heterogeneous reactions may be the dominant loss process for several atmospheric species, particularly late in the day and at night.

Several common atmospheric species thus react at a significant rate on bulk H_2SO_4 surfaces. At typical tropospheric aerosol concentrations, heterogeneous reactions may provide very important sinks or loss mechanisms for these species.

ALAN C. BALDWIN
DAVID M. GOLDEN
Chemical Kinetics Department,
SRI International,
Menlo Park, California 94025

References and Notes

1. B. J. Finlayson and J. N. Pitts, Jr., *Science* **192**, 111 (1976); *Chlorofluoromethanes and the Stratosphere*, R. Hudson, Ed. (NASA Reference Publication 1010, National Aeronautics and Space Administration, Washington, D.C., August 1977); *Halocarbons: Effects on Stratospheric Ozone* (Panel on Atmospheric Chemistry, National Research Council, Washington, D.C., 1976.
2. *Int. J. Chem. Kinet. Symp. No. 1* (1975).
3. For a general review of the experimental technique, see D. M. Golden, G. N. Spokes, S. W. Benson, *Angew. Chem. Int. Ed. Engl.* **12**, 534 (1973). The average molecule made either 10^3 or 10^4 collisions with the acid surface before leaving the reactor.
4. R. D. Cadle, *Eos (Trans. Am. Geophys. Union)* **53**, 812 (1972).
4a. _____, P. J. Crutzen, D. Ehhalt, *J. Geophys. Res.* **80**, 3381 (1975).
5. In this calculation, we followed the method of N. Davidson [*Statistical Mechanics* (McGraw-Hill, New York, 1962), p. 101], using aerosol data taken from (*2*).
6. The basis of this calculation is that the chemical characteristics of the aerosol particle are essentially the same as those of our bulk H_2SO_4 surface.
7. We monitored HNO_3 and N_2O_5 in terms of their mass peak at a mass-to-charge ratio (*m/e*) of 46; a product, presumably NO_2, also having a mass peak at *m/e* 46, formed in the reaction; thus the measured γ values were upper limits.
8. Water reacted almost completely within the minimum number of collisions obtainable with our present apparatus.
9. In our system, NH_3 reacted completely; γ may be much larger than 10^{-3}.
10. Supported was provided by the Division of Biomedical and Environmental Research, Department of Energy, under contract EP-78-C-03-2109; additional support was obtained from the National Aeronautics and Space Administration under contract 954815.

26 April 1979; revised 29 June 1979

Morphologies and Origin of Elemental Carbon in the Environment

Abstract. *Carbon particles extracted from sediments collected by box coring from southeastern Lake Michigan were compared with carbon particles extracted from oil, coal, and wood fly ash. Sediments deposited after 1900 contained coal, oil, and wood carbons; older sediments contained only wood carbon.*

A measure of the relative intensities of fossil-fuel burning (coal, oil, and natural gas) and of wood burning, both natural and man-instigated, is found in the amounts of the combustion products. Both the organic compounds and the elemental carbon particles may be characteristic of the burned materials, based either on their compositions or on the parameters of the combustion. Under

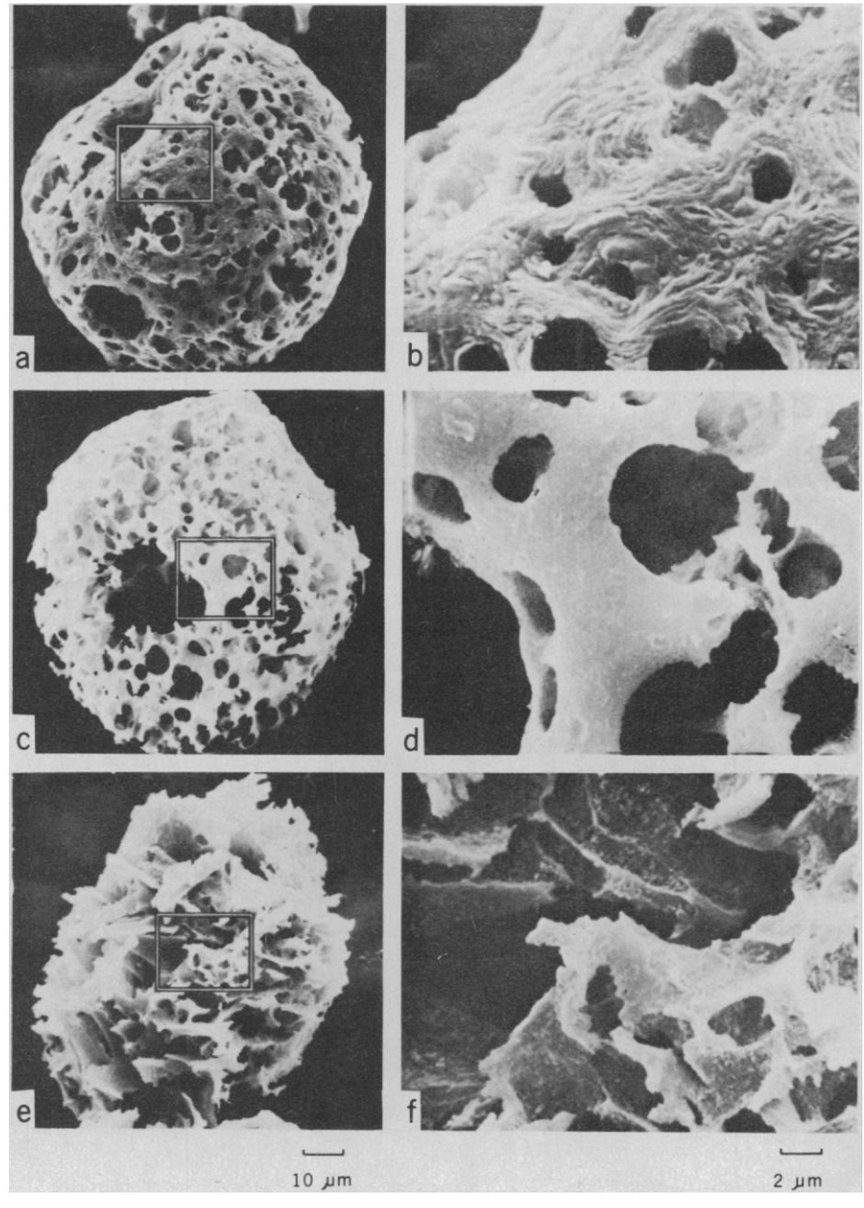

Fig. 1. Scanning electron micrographs of the carbon particles used as standards in this study: (left) single cenosphere; (right) higher magnification close-up of the surface area inside the square outlined at left. The oil carbon particles (a and b) were extracted from fly ash provided by the Florida Power and Light Company and collected from the dust collector of a oil-fired power plant. The coal carbon particles (c and d) were extracted from fly ash provided by the city of St. Louis, Missouri, and collected from the electrostatic precipitator of a pulverized coal-fired power plant. The wood carbon particles (e and f) were extracted from material taken from the flue of a residential wood-burning fireplace.

0036-8075/79/1102-0563$00.50/0

favorable conditions these combustion products are deposited in sediments and are preserved to yield a historical record of burning (*1*, *2*).

We have examined by scanning electron microscopy and light microscopy the carbon particles produced in the burning of coal, oil, and wood. Morphological differences in carbon particles produced in coal burning and charring have been studied (*3*). The carbon particles resulting from oil burning have a unique fine structure which does not appear in the carbon from the burning of coal or wood (Fig. 1). The surface of the oil carbon shows a convoluted, layered structure, whereas the surfaces of the coal and wood carbons are homogeneous, with little characteristic fine structure that would be useful for identification purposes. The fine structure exhibited by the oil carbons may be related to the nature of the liquid droplets atomized into the combustion chamber and the temperatures therein, whereas the homogeneous structure of the coal and wood carbons is apparently determined by the characteristics of the burning process, such as temperature (*3*).

Some coal carbons show a distinct remnant wood structure, making them difficult to distinguish from wood carbons. Plant materials, in general, are thought to be precursors of coal, and during combustion some of the coalified plant parts apparently disintegrate along the original structures, yielding fairly well preserved plant morphologies in the coal carbon particles (Fig. 2).

Under the light microscope the oil carbons usually showed cenospheres with delicate, lacy network structures. In contrast, the coal carbons consisted mostly of fragments with few cenospheres. Their network structures were more robust and not as delicate and lacy, whereas the wood carbon often exhibited some indication of plant structure and had a ratio of length to width greater than 3. We gained additional confidence in our ability to distinguish coal from wood carbons from the analysis of samples that had associated unburned coal particles or had partially carbonized wood fragments.

Using the most distinguishing microscopic characteristics of the oil, coal, and wood carbons, we have examined the carbon particles extracted from sediment obtained from a box core taken from southeastern Lake Michigan (*4*). There is a significant transition in the sources of carbon at a depth of 30 cm which corresponds in time to about 1900 (Table 1). Above the transition, oil and coal carbons are abundant. We attribute sources for the oil and coal carbons to industrial activity which grew dramatically during the 20th century. Below 30 cm, wood carbon and pollen grains are abundant. The "wood" carbon has certainly been produced from the natural and anthropogenic combustion of woods and grasses. A similar increase in the concentrations of polycyclic aromatic hydrocarbons has been observed in sediments from Buzzards Bay, Massachusetts, between 1850 and 1900 and attributed to increases in coal and oil burning (*2*).

We have extracted the carbon particles from an air sample collected during March 1970 at the Scripps Institution of Oceanography Pier, La Jolla, California. The composition of the particles were as follows: 36 percent wood carbon, 16 percent oil carbon, 5 percent unidentifiable carbon, and 43 percent pollen grains. The results suggest that forest and grass

Table 1. Relative percentages of wood, oil, and coal carbon particles and pollen grains in a Lake Michigan core (*4*).

Depth (cm)	Year of deposition*	Number of particles analyzed†	Wood carbon (%)	Coal carbon (%)	Oil carbon (%)	Miscellaneous carbon (%)	Pollen grains (%)
0-10	1953-1978	1480	9.0	68	13	0	10
10-20	1928-1953	1692	8.6	62	6.4	0.1	23
20-30	1903-1928	1601	18	42	1.6	0	38
30-40	1878-1903	2324	33	Trace	0	0.3	67
40-50	1853-1878	2697	39	Trace	Trace	0.5	60
50-60	1828-1853	808	37	0	0	0.7	62

*Chronology was established by a ^{210}Pb technique (*5*). †The identification of carbon type and the particle count were done with a light microscope equipped with a mechanical stage. We computed the total particle counts by noting each particle intersecting the crosshair of the microscope eyepiece while scanning a 5-cm^2 area of the slide.

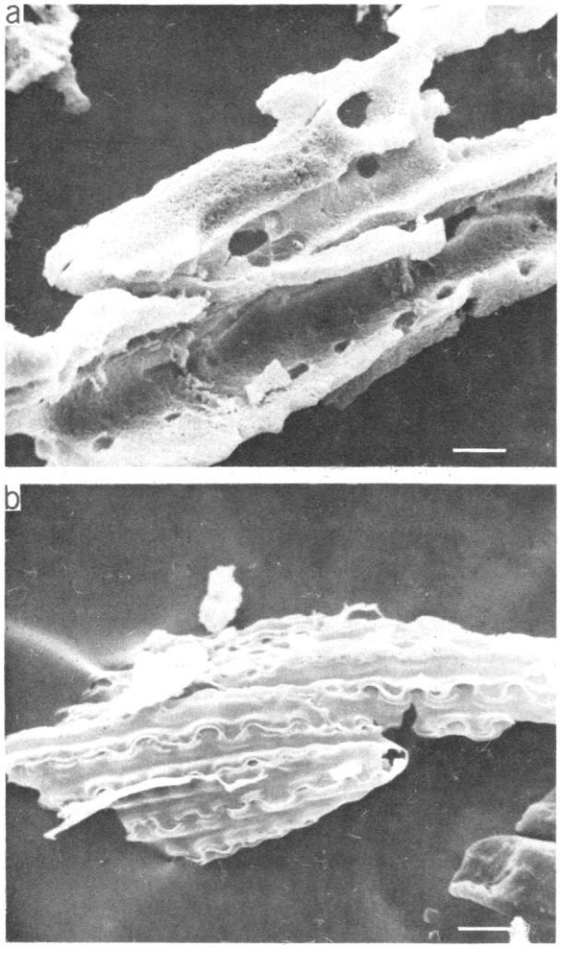

Fig. 2. Scanning electron micrographs of coal and wood carbon particles: (a) coal carbon particle extracted from fly ash obtained from a chain-grate, stocker-fired boiler, fueled with 3-cm coal. (b) Plant carbon particle extracted from sediment sampled from the 50- to 60-cm section of the Lake Michigan core. Note the morphological similarities between the coal and the plant carbon particles. These same general structural features, common to plants, also were noted in some carbon particles extracted from fly ash obtained from power plants that burn pulverized coal. Scale equals 10 μm.

burning in this area can be significant sources of carbon that contribute to the atmospheric particulate carbon burden.

The type and concentration of carbon particles in sediments not only may provide historical records of natural and anthropogenic burning but also may act as indicators of other substances such as metals and organics mobilized to the environment during the combustions. Finally, examination of the types, dimensions, and amounts of carbon particles deposited over the past decades will indicate how effective are the pollution control devices that have been installed on plants producing energy from fossil fuels.

JOHN J. GRIFFIN
EDWARD D. GOLDBERG
Scripps Institution of Oceanography, University of California, San Diego, La Jolla 92093

References and Notes

1. D. W. Smith, J. J. Griffin, E. D. Goldberg, *Nature (London)* **241**, 268 (1973); A.M. Swain, *Quat. Res. (N.Y.)* **3**, 383 (19 → J. J. Griffin and E. D. Goldberg, *Limnol. Oceanogr.* **20**, 456 (1975); W. W. Youngblood and M. Blumer, *Geochim. Cosmochim. Acta* **39**, 1303 (1975); J. R. Herring, thesis, University of California, San Diego (1977); G. Müeller, G. Grimmer, H. Böhnke, *Naturwissenschaften* **64**, 427 (1977); G. Grimmer and H. Böhnke, *Cancer Lett.* **1**, 75 (1975).
2. R. A. Hites, R. E. Laflamme, J. W. Farrington, *Science* **198**, 829 (1977).
3. P. Lightman and P. J. Street, *Fuel* **47**, 7 (1968).
4. Box core LM-780914 was located at 43°00′N, 86°22′W; water depth, 64 m. The carbon particles were extracted by a combination of chemical and physical methods. All samples, including the standards, were acid-digested with HF-HCl and then were oxidized with KOH-H_2O_2. The residues were sieved and density-separated to yield a < 38-μm fraction with a density of < 2.3 g/cm^3 for study under the microscope.
5. M. Koide, K. W. Bruland, E. D. Goldberg, *Geochim. Cosmochim. Acta* **37**, 1171 (1973).
6. This work was supported by grant DOE EY-76-S-03-0034, PA 84 with the Division of Biology and Medicine, Environmental Sciences Branch, Energy Research and Development Administration, Department of Energy.

1 March 1979; revised 4 May 1979

End-Capillary Loops in the Heart: An Explanation for Discrete Myocardial Infarctions Without Border Zones

Abstract. *Separate perfusions of canine coronary arteries with colored silicone-rubber compound reveal that in the region where two microcirculations abut, capillaries derived from individual large vessels are discrete, with no interconnections. Terminal homologous capillaries form loops rather than anastomosing with heterologous capillaries. This anatomic arrangement may account for discrete myocardial infarctions without ischemic border zones.*

Studies from our laboratory have shown that the amount of myocardium susceptible to necrosis is determined by the volume perfused by the vessel supplying that tissue. These investigations revealed a homogeneous necrotic zone, with uniform depletion of creatine kinase from the central to the lateral edge of the infarction (*1*). No lateral border zone of intermediate depletion could be demonstrated when tissue supplied by the nonoccluded vessel was excluded from analysis. Histologically, a serial-section study of acute canine myocardial infarctions demonstrated that the boundary between necrotic and normal tissue at the lateral edge of an infarction was composed of a remarkably complex interdigitation of discrete tissue, with no identifiable border zone of ischemic but viable myocardium (*2*). More recently, we extended the serial-section analysis by doubly injecting the occluded left anterior descending coronary artery (LAD) and the nonoccluded main left coronary artery (or nonoccluded LAD branch) with white and red silicone rubber (Microfil), respectively. We were able to show that all necrotic myocardium was supplied by the LAD; the surrounding normal myocardium was supplied by the main left or nonoccluded LAD branch (*3*).

Although the concept that the myocardium at risk is equal to the volume of tissue perfused by the occluded vessel appears obvious, it conflicts with the commonly accepted "bull's-eye" view of myocardial infarction: an area of central necrosis, surrounded by a border zone of ischemic but viable tissue, which blends imperceptibly into normal myocardium (*4*). The ischemic zone has been inferred from electrophysiological and biochemical data demonstrating intermediate levels of ST-segment elevation and depletion of creatine kinase in this region when compared to normal and necrotic tissue (*5*). We interpret this intermediate zone as an artifact derived from the summation of discrete normal and infarcted tissue peninsulas in the measured samples of myocardium (*1*, *2*). These peninsulas are so interdigitated along the lateral boundary of an infarction that manual or visual separation of tissue is impossible.

Proponents of the bull's-eye view of myocardial infarction have not addressed the issue of what anatomic arrangement of the microvasculature could account for an ischemic border zone. Two arrangements of the vessels are conceivable. In one, complex alternation of capillaries derived from both the occluded and nonoccluded coronary arteries would allow individual cells to be perfused by both circulations. In the other, a network of existing precapillary and capillary anastomoses between vessels derived from occluded and nonoccluded coronary arteries could provide sufficient blood flow at the border to maintain viability of ischemic tissue. Although extensive preformed collateral networks between larger vessels exist in many species (*6*–*8*), anastomoses of small caliber vessels in the mammalian heart have rarely been mentioned (*9*). Most studies of the coronary vasculature utilized technology that precluded analysis of vessels below arteriolar size (*6*, *8*). The purpose of the study reported here was to characterize the anatomic arrangement of the normal microcirculation in the region where two vascular networks supplied by separate coronary arteries or branches of a single coronary artery interdigitate. This area would be equivalent to the lateral border zone if myocardial infarction were present.

Four mongrel dogs had white Microfil injected into the LAD; simultaneously, and under equal pressure, red Microfil was injected into an artery perfusing an adjacent region: either the main left or a proximal branch of the LAD (two dogs each). In seven other dogs white Microfil was injected into the LAD, red into a proximal branch, and yellow into the LAD proximal to the branch. In one dog white Microfil was injected only into the LAD. The entire heart was cleared with organic solvents as described by Schaper (*8*). After several weeks, the hearts were semitranslucent and amber, with colored zones corresponding to the filled capillary networks. Portions of tissue 1 to 2 mm thick were removed freehand from the boundary of the two circulations. Sections oblique to the longitudinal axis of the vessels as visualized under a dissecting microscope were taken. The tissue slices were examined with epi-illumination under the ×2.5 and ×6.3 objectives of a standard photomicroscope to permit color characterization of the vessels.

The entire depth of the tissue slices was visualized with appropriate focusing, and individual vessels could be followed for relatively long distances. The capillary beds were remarkably discrete

0036-8075/79/1102-0565$00.50/0